

Supplementary Information

Complex Crystal Structures of EGFR With Third-Generation Kinase Inhibitors and Simultaneously Bound Allosteric Ligands

Janina Niggenaber, Leonie Heyden, Tobias Grabe, Matthias P. Müller, Jonas Lategahn, Daniel Rauh*

Abstract: Osimertinib is a third-generation tyrosine kinase inhibitor (TKI) and currently the gold-standard for the treatment of patients suffering from non-small cell lung cancer (NSCLC) harboring T790M-mutated epidermal growth factor receptor (EGFR). The outcome of the treatment, however, is limited by the emergence of the C797S resistance mutation. Allosteric inhibitors have a different mode of action and were developed to overcome this limitation. However, most of these innovative molecules are not effective as a single agent. Recently, mutated EGFR was successfully addressed with osimertinib combined with the allosteric inhibitor JBJ-04-125-02, but surprisingly, structural insights into their binding mode were lacking. Here, we present the first complex crystal structures of mutant EGFR in complex with third-generation inhibitors such as osimertinib and mavelertinib in the presence of simultaneously bound allosteric inhibitors. These structures highlight the possibility of further combinations targeting EGFR and lay the foundation for hybrid inhibitors as next-generation TKIs.

TABLE OF CONTENTS

Figure S1: Structural alignment of allosteric inhibitors and detailed overview of two published structures of osimertinib bound to EGFR-T790M	S3
Figure S2: Detailed overview of complex crystal structure of osimertinib and EAI045 bound to EGFR-T790M/V948R	S4
Figure S3: Detailed overview of complex crystal structure of mavelertinib and EAI001 bound to EGFR-T790M/V948R	S5
Figure S4: Detailed overview of complex crystal structure of spebrutinib and EAI001 bound to EGFR-T790M/V948R	S6
Figure S5: Mass spectra of apo EGFR-T790M/V948R and EGFR-T790M/V948R incubated with osimertinib, mavelertinib or spebrutinib	S7
Figure S6: Superposition of the EAI001 bound to EGFR-T790M/V948R	S8
Figure S7: Structural alignment of the complex crystal structures of osimertinib, mavelertinib, and spebrutinib simultaneously bound with allosteric inhibitors to EGFR-T790M/V948R	S9
Table S1: Data collection and refinement statistics of complex crystal structures	S10
Experimental Procedures	S12

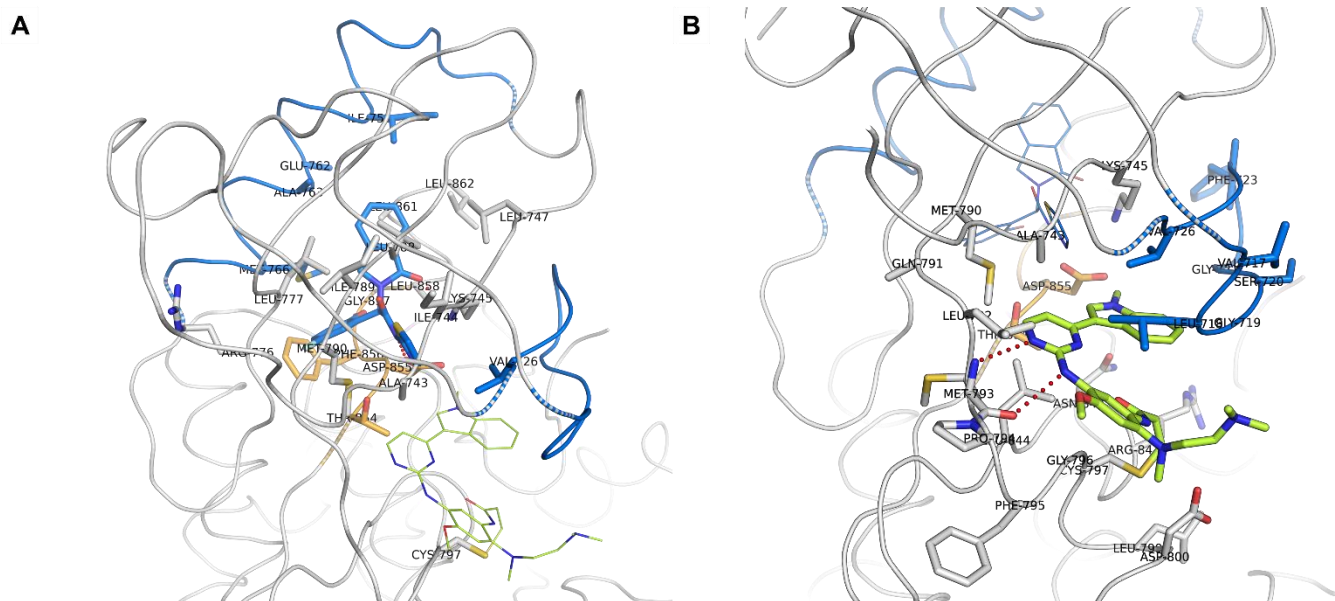


Figure S2. Detailed overview of complex crystal structure of osimertinib and EAI045 bound to EGFR-T790M/V948R. **(A)** Detailed interactions of EAI045 bound together with osimertinib to EGFR-T790M/V948R (chain A & B) (PDB-ID: 6Z4B). Residues within 5 Å are shown. **(B)** Detailed interactions of osimertinib bound together with EAI045 to EGFR-T790M/V948R (chain A & B) (PDB-ID: 6Z4B). Residues within 5 Å are shown.

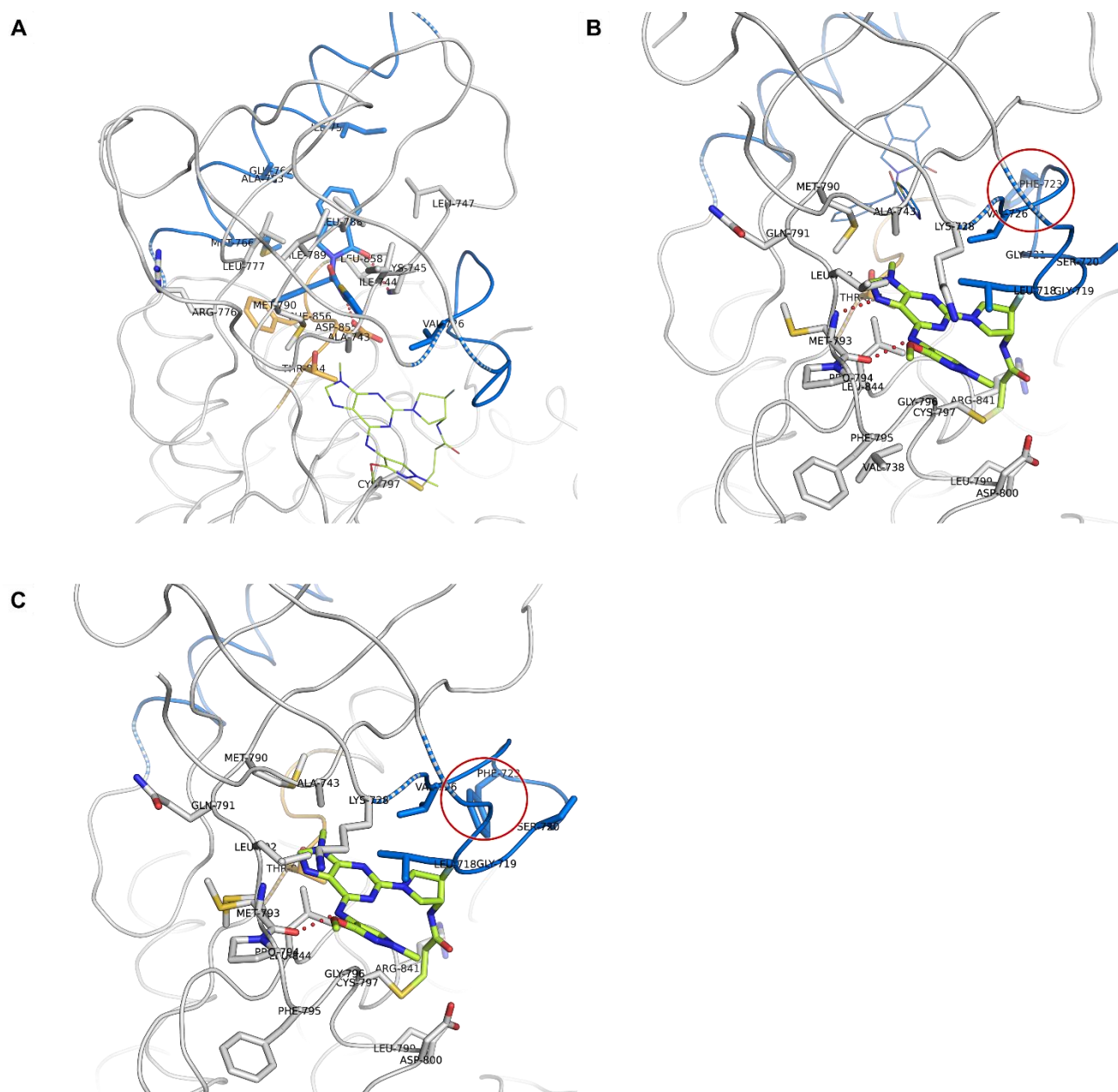


Figure S3. Detailed overview of complex crystal structure of mavelertinib and EAI001 bound to EGFR-T790M/V948R. **(A)** Detailed interactions of EAI001 bound together with mavelertinib to EGFR-T790M/V948R (chain B) (PDB-ID: 6Z4D). Residues within 5 Å are shown. **(B)** Detailed interactions of mavelertinib bound together with EAI001 to EGFR-T790M/V948R (chain B) (PDB-ID: 6Z4D) Residues within 5 Å are shown. **(C)** Detailed interactions in of mavelertinib bound to EGFR-T790M/V948R without simultaneously bound EAI001 (chain A) (PDB-ID: 6Z4D) Residues within 5 Å are shown. Phe723 is marked with red circles to highlight the different orientations of the residue.

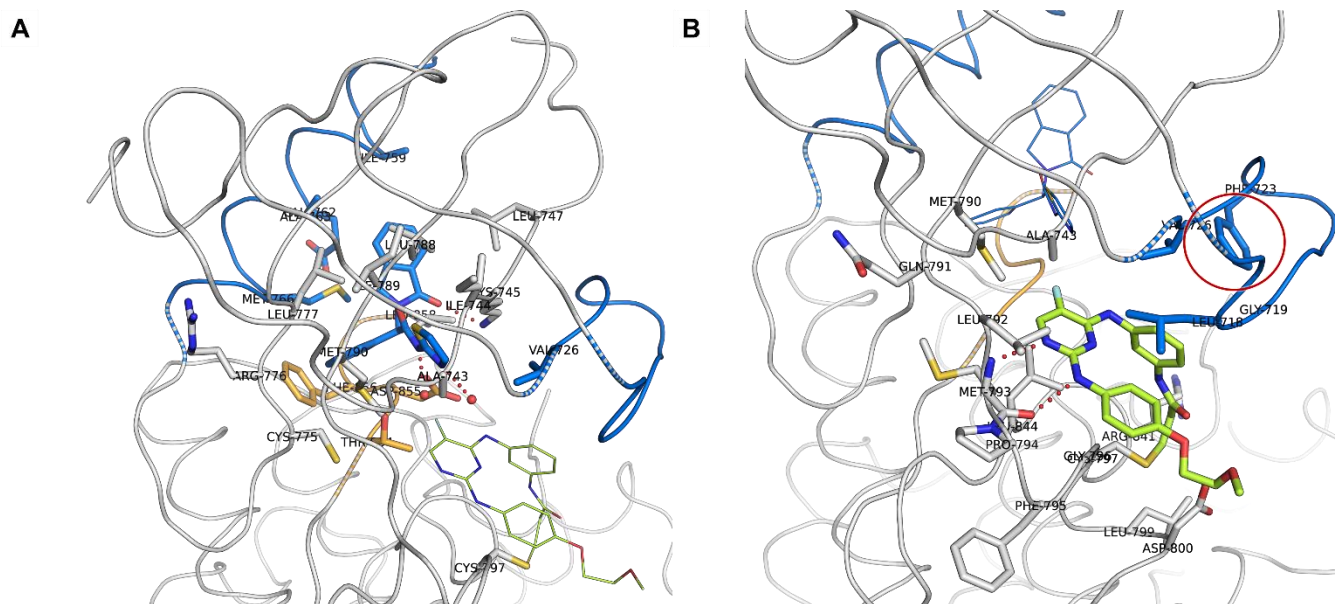


Figure S4. Detailed overview of complex crystal structure of spebrutinib and EAI001 bound to EGFR-T790M/V948R. **(A)** Detailed interactions of EAI001 bound together with spebrutinib to EGFR-T790M/V948R (chain A & B) (PDB-ID: 7A2A). Residues within 5 Å are shown. **(B)** Detailed interactions of spebrutinib bound together with EAI001 to EGFR-T790M/V948R (chain A & B) (PDB-ID: 7A2A). Residues within 5 Å are shown. Phe723 is marked with red circles to highlight the different orientations of the residue.

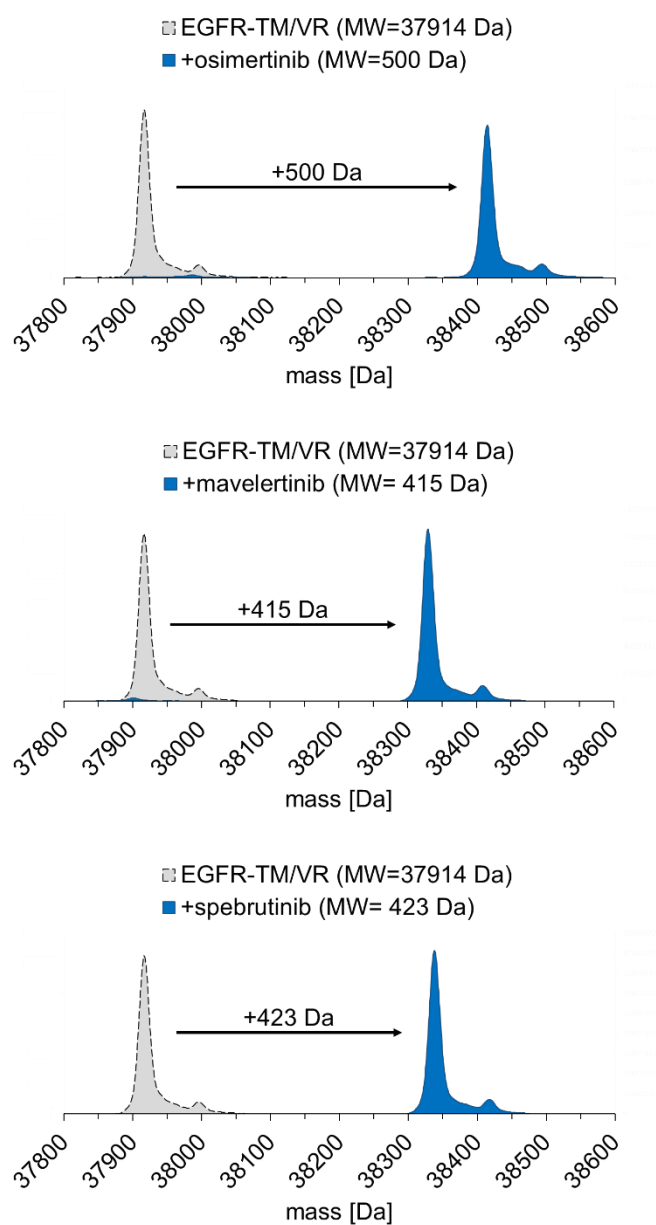


Figure S5. Mass spectra of apo EGFR-T790M/V948R (gray) and EGFR-T790M/V948R incubated with osimertinib, mavelertinib or spebrutinib (blue).

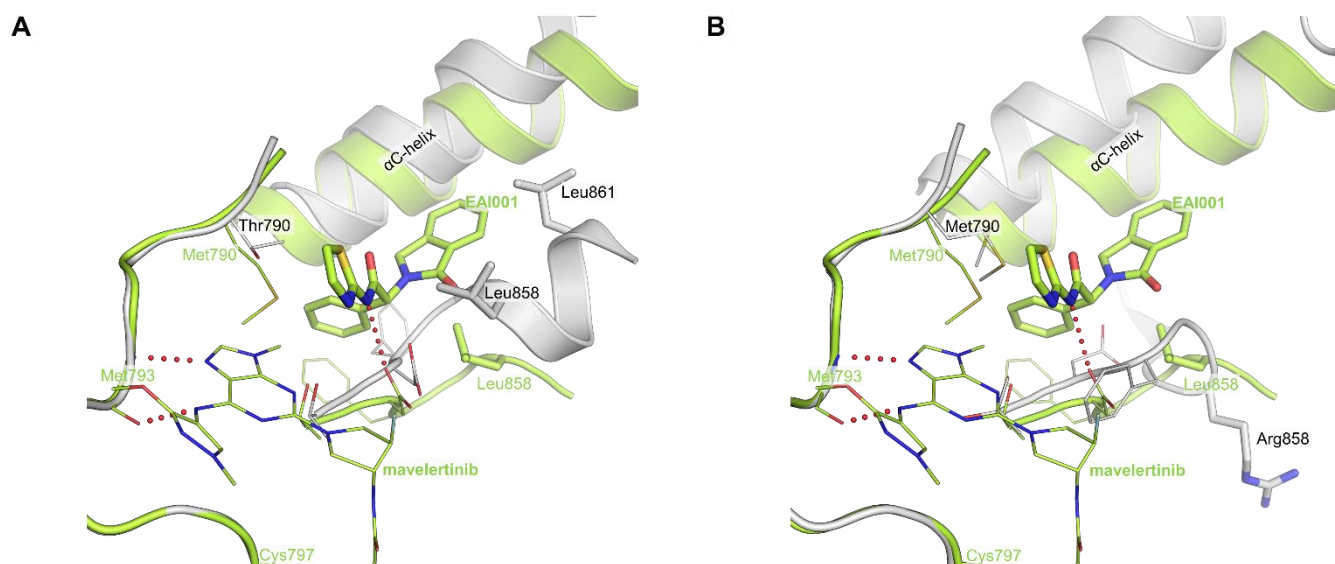


Figure S6. Superposition of the EAI001 bound to EGFR-T790M/V948R with the inactive conformation of wild type EGFR and with EGFR-L858R/T790M/V948R. (A) Superposition of EAI001 bound to EGFR-T790M/V948R (PDB-ID: 6Z4D, green structure) and the inactive conformation of wild type EGFR (PDB-ID: 2GS7, gray structure). The allosteric inhibitor cannot bind the inactive state of wild type EGFR because of steric clashes with side chains of Leu858 and Leu861 (gray residues). These two leucine residues lie in a short helical area of the activation loop. (B) Superposition of EAI001 bound to EGFR-T790M/V948R (PDB-ID: 6Z4D, green structure) and EGFR-L858R/T790M/V948R (PDB-ID: 5HG5, gray structure). However, the L858R mutation, which disrupts the short helical element of the activation loop of the inactive kinase conformation, is required for allosteric inhibitor binding, the EAI001 induces the reposition of Leu858 and this induces a structural change of the helical element of the activation loop. Therefore, Leu858 contributes to the hydrophobic framework of EAI001 but does not clash with the inhibitor.

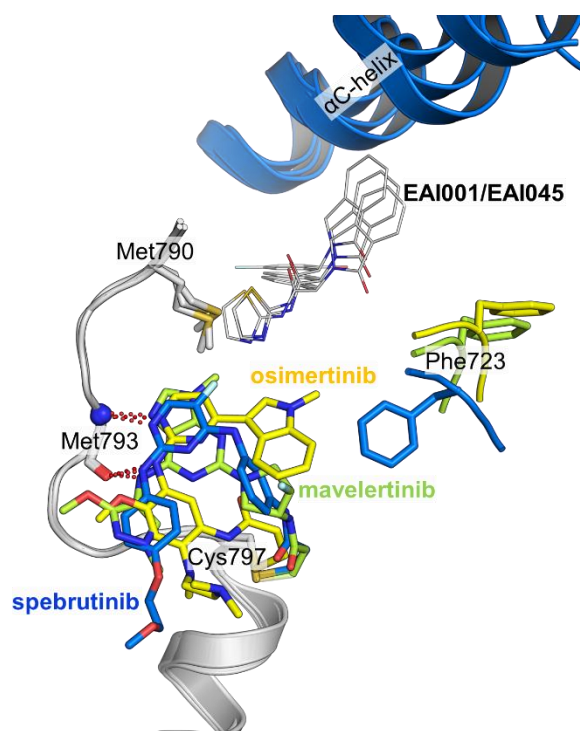


Figure S7. Structural alignment of the complex crystal structures of osimertinib, mavelertinib, and spebrutinib simultaneously bound with allosteric inhibitors to EGFR-T790M/V948R. In the structure of spebrutinib and EAI001 bound to EGFR-T790M/V948R (PDB-ID: 7A2A), the Phe723 (blue) is flipped towards spebrutinib (blue) and contributing to the hydrophobic framework, although, the allosteric inhibitor is bound. This can be explained by the lower steric demand of spebrutinib in the ATP-binding pocket. In the structure of mavelertinib and EAI001(PDB-ID: 6Z4D) as well as osimertinib and EAI045 (PDB-ID: 6Z4B) bound to EGFR-T790M/V948R Phe723 (yellow and green) flipped into the other direction and does not contribute to the hydrophobic framework of osimertinib (yellow) and mavelertinib (green).

Table S1. Data collection and refinement statistics of complex crystal structures.^a

	EGFR-T790M/V948R + osimertinib + EAI045 PDB-ID: 6Z4B	EGFR-T790M/V948R + mavelertinib + EAI001 PDB-ID: 6Z4D	EGFR-T790M/V948R + spebrutinib + EAI001 PDB-ID: 7A2A
Data collection			
Space group	P 2(1) 2(1) 2(1) (19)	P 2(1) 2(1) 2(1) (19)	P 2(1) 2(1) 2(1) (19)
Cell dimensions			
a, b, c [Å]	76.20, 79.70, 89.20	76.61, 83.90, 89.27	75.18, 83.73, 92.34
α, β, γ [°]	90.00, 90.00, 90.00	90.00, 90.00, 90.00	90.00, 90.00, 90.00
Resolution [Å]	44.60-2.50 (2.60-2.50)	47.79-2.00 (2.10-2.00)	47.84-1.90 (2.00-1.90)
R_{meas} [%]	10.9 (108.5)	9.1 (164.8)	6.3 (169.8)
<i>I</i> / σI	11.15 (1.92)	16.12 (1.80)	21.34 (2.09)
Completeness [%]	100.0 (99.9)	100.0 (100.0)	100.0 (100.0)
CC_{1/2}	99.8 (69.5)	99.9 (78.0)	99.9 (74.6)
Redundancy	6.57 (6.49)	13.44 (13.75)	13.27 (14.16)
Refinement			
Resolution [Å]	44.60-2.50 (2.60-2.50)	47.79-2.00 (2.10-2.00)	47.84-1.90 (2.00-1.90)
No. reflections	19371	39566	46627
R_{work} / R_{free}	22.07 / 25.13 (30.57 / 31.45)	19.31 / 22.14 (31.38 / 37.50)	19.43 / 21.71 (30.45 / 30.27)
No. atoms			
Protein	4122 (chain A=2093; chain B=2029)	4216 (chain A=2127; chain B=2089)	4136 (chain A=2055; chain B=2081)
Covalent Ligand	74 (chain A=37; chain B=37)	60 (chain A=30; chain B=30)	62 (chain A=31; chain B=31)
Ion	50	25	20
Allosteric Ligand	54	25	50

	EGFR-T790M/V948R + osimertinib + EAI045 PDB-ID: 6Z4B	EGFR-T790M/V948R + mavelertinib + EAI001 PDB-ID: 6Z4D	EGFR-T790M/V948R + spebrutinib + EAI001 PDB-ID: 7A2A
	(chain A=27; chain B=27)	(chain A=not present; chain B=25)	(chain A=25; chain B=25)
Water	25	174	116
B-factors			
Protein	59.09 (chain A=55.12; chain B=63.05)	52.12 (chain A=48.82; chain B=55.41)	57.98 (chain A=53.39; chain B=62.57)
Covalent Ligand	51.07 (chain A=47.29; chain B=54.85)	43.56 (chain A=46.09; chain B=41.03)	53.78 (chain A=55.38; chain B=52.18)
Ion	105.96	98.74	85.42
Allosteric Ligand	52.15 (chain A=49.46; chain B=54.84)	50.91 (chain A=not present; chain B=50.91)	46.54 (chain A=48.53; chain B=44.54)
Water	51.14	51.77	55.16
R.m.s. deviations			
Bond lengths [Å]	0.004	0.003	0.006
Bond angles [°]	0.806	0.609	0.855
Ramachandran plot			
Ramachandran outliers [%]	0.00	0.00	0.00
Ramachandran allowed [%]	1.53	1.51	1.53
Ramachandran favored [%]	98.47	98.49	98.47

^aDiffraction data from a single crystal was used to determine the complex structure. Values in parenthesis are referring to the highest resolution shell.

Experimental Procedures

Construct Design of EGFR-T790M/V948R.

For crystallographic studies, codon-optimized DNA encoding residues 696-1022 of the human EGFR with a N-terminal His6-tag and thrombin cleavage site was cloned into a pIEX/Bac-3 vector. Point mutations T790M and V948R were introduced by site-directed mutagenesis (QuikChange, Stratagene/Agilent Technologies). Transfection, virus generation, amplification, and expression were carried out in *Spodoptera frugiperda* cell line Sf9 following the flashBAC protocol.

Protein Expression and Purification.

After three days of expression (27 °C, 110 rpm) the Sf9-cells were harvested (3000 g, 20 min), resuspended in lysis buffer (600 mM NaCl, 50 mM Tris-HCl pH 7.5, 15% glycerol, 1 mM TCEP) supplemented with a protease-inhibitor cocktail (Complete EDTA-free), homogenized, lysed and incubated with CHAPS (1 h, 4 °C) followed by centrifugation (20500 rpm, 1 h, 4 °C). The filtered supernatant was loaded onto a nickel-affinity column. The protein was eluted with 500 mM NaCl, 25 mM Tris-HCl pH 8, 250 mM imidazole, 10% glycerol, and 1 mM TCEP followed by cleavage with thrombin to remove the His6-tag and a second nickel-affinity chromatography capturing the flow through. Finally, the protein was purified by size-exclusion chromatography (100 mM NaCl, 25 mM Tris-HCl pH 8, 10% glycerol, and 1 mM TCEP) and concentrated to 4.7-5.0 mg/mL. Protein identity was confirmed by ESI-MS analysis.

Crystallization of EGFR-T790M/V948R.

The concentrated protein EGFR-T790M/V948R (4.7-5.0 mg/mL) was incubated with a one- to three-fold excess of ATP-competitive inhibitors osimertinib or mavelertinib or spebrutinib (10 mM DMSO stock) together with one- to two-fold excess of allosteric inhibitors EAI001 or EAI045 (10 mM DMSO stock) for 2 h on ice. Crystals were grown at 20 °C by hanging drop vapor diffusion method. The protein-compound-complex was mixed in a 1:1 ratio (1 µL protein and 1 µL reservoir solution containing 15-37.5% PEG3350, 100-200 mM MgSO₄, 0-4% ethylene glycol). Crystals grew within one to two weeks and were harvested and flash-cooled in liquid nitrogen. Diffraction data were collected at the PXII X10SA beamline at the Swiss Light Source (PSI, Villigen, Switzerland). The data were processed using XDS and scaled using XSCALE (W. Kabsch, XDS. Acta Cryst. 2010, D66, 125-132).

Structure Determination and Refinement.

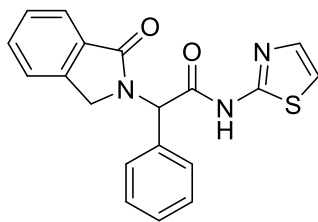
The complex crystal structures of EGFR-T790M/V948R were solved by molecular replacement with PHASER (R.J. Read, Acta Crystallogr D Biol Crystallogr 2001, 57, 1373-1382) using structure PDB ID:

6S8A as template. The molecules in the asymmetric unit were manually adjusted using the program COOT (P. Emsley, K. Cowtan, *Acta Crystallogr D Biol Crystallogr* 2004, 60, 2126-2132). The refinement was performed with Phenix.refine 1.17.1 (P.D. Adams, P.V. Afonine, G. Bunkoczi, V.B. Chen, I.W. Davis, N. Echols, J.J. Headd, L.W. Hung, G.J. Kapral, R.W. Grosse-Kunstleve, A.J. McCoy, N.W. Moriarty, R. Oeffner, R.J. Read, D.C. Richardson, J.S. Richardson, T.C. Terwilliger, P.H. Zwart, *Acta Cryst* 2010, D66, 213-221). Inhibitor topology files were generated using eLBOW of the Phenix1.17.1 program package. Refined structures were validated with the PDB validation server. Data collection, structure refinement statistics, PDB-ID codes, and further details for data collection are provided in Table S1. PyMOL (W.L. DeLano, The PyMOL Molecular Graphics System) was used for generating the figures.

Mass spectrometry experiments.

The concentrated protein EGFR-T790M/V948R (1.0 mg/mL) was incubated with a three-fold excess of osimertinib, mavelertinib and spebrutinib or with a one- to three-fold excess of ATP-competitive inhibitors osimertinib, mavelertinib and spebrutinib (10 mM DMSO stock) together with one- to two-fold excess of allosteric inhibitors EAI001 or EAI045 (10 mM DMSO stock) for 1-2 h on ice in buffer (100 mM NaCl, 25 mM Tris-HCl, 10% glycerol and 1 mM TCEP, pH 8.0). We analyzed the aliquots by ESI-MS using a Thermo Fisher Scientific Dionex UltiMate 3000 HPLC system connected to a Thermo Fisher Scientific Velos Pro (2d ion trap). Therefore, 2 μ L of the sample was injected and separated using a Vydac 214TP C4 5 μ m column (150 mm x 2.1 mm) starting at 20% of solvent B for 5 minutes followed by a gradient up to 90% of solvent B over 14 min with a flow rate of 210 μ L/min with 0.1% TFA in water as solvent A and 0.1% TFA in MeCN as solvent B. A mass range of 700 to 2000 m/z was scanned and raw data were deconvoluted and analyzed with MagTran software (Z.Q. Zhang, A.G. Marshall, *J. Am. Soc. Mass. Spectr.* 1998, 9, 225-233).

Synthesis and characterization of EAI001 – 2-(1-oxoisindolin-2-yl)-2-phenyl-N-(thiazol-2-yl)acetamide.



The synthesis was derived from the described route (J.C. Breytenbach et al. *Bioorg. Med. Chem. Lett.* **2000**, 10, 1629-1631). This final compound was purified to $\geq 95\%$ purity confirmed by NMR analysis as well as LC/MS analysis on LCQ Advantage MAX (1200series, Agilent) with Eclipse XDB-C18-column (5 μ M 150 \times 1.6mm, Phenomenex) or Agilent Technologies 1100 HPLC system (Macherey Nagel 125/4 Nucleodur C18 Gravity, 3 μ M column).

^1H NMR (500 MHz, DMSO- d_6) δ 3.98 (d, $J=17.40$ Hz, 1H) 4.76 (d, $J=17.40$ Hz, 1H) 6.32 (s, 1H) 7.28 (d, $J=3.42$ Hz, 1H) 7.36-7.53 (m, 7H) 7.54-7.63 (m, 2H) 7.74 (d, $J=7.83$ Hz, 1H) 12.70 ppm (s, 1H). **^{13}C NMR** (126 MHz, DMSO- d_6) δ 48.52, 58.11, 114.04, 122.92, 123.64, 127.96, 128.69, 128.76, 129.05, 131.36, 131.74, 134.43, 137.87, 142.37, 157.38, 167.71, 168.36 ppm. **HR-MS** (ESI+) m/z calculated for $[\text{C}_{19}\text{H}_{15}\text{N}_3\text{O}_2\text{S}+\text{H}]^+$ 350.0958, found 350.0964.

EAI045, osimertinib, mavelertinib and spebrutinib were purchased from commercial vendors.